

A new embedding quality assessment method for manifold learning

Peng Zhang *Member, IEEE*, Yuanyuan Ren, and Bo Zhang

Abstract—Manifold learning is a hot research topic in the field of computer science. A crucial issue with current manifold learning methods is that they lack a natural quantitative measure to assess the quality of learned embeddings, which greatly limits their applications to real-world problems. In this paper, a new embedding quality assessment method for manifold learning, named as Normalization Independent Embedding Quality Assessment (NIEQA), is proposed. Compared with current assessment methods which are limited to isometric embeddings, the NIEQA method has a much larger application range due to two features. First, it is based on a new measure which can effectively evaluate how well local neighborhood geometry is preserved under normalization, hence it can be applied to both isometric and normalized embeddings. Second, it can provide both local and global evaluations to output an overall assessment. Therefore, NIEQA can serve as a natural tool in model selection and evaluation tasks for manifold learning. Experimental results on benchmark data sets validate the effectiveness of the proposed method.

Index Terms—Nonlinear Dimensionality reduction, Manifold learning, Data analysis

I. INTRODUCTION

ALONG with the advance of techniques to collect and store large sets of high-dimensional data, how to efficiently process such data issues a challenge for many fields in computer science, such as pattern recognition, visual understanding and data mining. The key problem is caused by “the curse of dimensionality” [1], that is, in handling with such data the computational complexities of algorithms often go up exponentially with the dimension.

The main approach to address this issue is to perform dimensionality reduction. Classical linear methods, such as Principal Component Analysis (PCA) [2], [3] and Multidimensional Scaling (MDS) [4], achieve their success under the assumption that data lie in a linear subspace. However, such assumption may not usually hold and a more realistic assumption is that data lie on or close to a low-dimensional

manifold embedded in the high-dimensional ambient space. Recently, many methods have been proposed to efficiently find meaningful low-dimensional embeddings from manifold-modeled data, and they form a family of dimensionality reduction methods called *manifold learning*. Representative methods include Locally Linear Embedding (LLE) [5], [6], ISOMAP [7], [8], Laplacian Eigenmap (LE) [9], [10], Hessian LLE (HLLE) [11], Diffusion Maps (DM) [12], [13], Local Tangent Space Alignment (LTSA) [14], Maximum Variance Unfolding (MVU) [15], and Riemannian Manifold Learning (RML) [16].

Manifold learning methods have drawn great research interests due to their nonlinear nature, simple intuition, and computational simplicity. They also have many successful applications, such as motion detection [17], sample preprocessing [18], gait analysis [19], facial expression recognition [20], hyperspectral imagery processing [21], and visual tracking [22].

Despite the above success, a crucial issue with current manifold learning methods is that they lack a natural measure to assess the quality of learned embeddings. In supervised learning tasks such as classification, the classification rate can be directly obtained through label information and used as a natural tool to evaluate the performance of the classifier. However, manifold learning methods are fully unsupervised and the intrinsic degrees of freedom underlying high-dimensional data are unknown. Therefore, after training process, we can not directly assess the quality of the learned embedding. As a consequence, model selection and model evaluation are infeasible. Although visual inspection on the embedding may be an intuitive and qualitative assessment, it can not provide a quantitative evaluation. Moreover, it can not be used for embeddings whose dimensions are larger than three.

Recently, several approaches have been proposed to address the issue of embedding quality assessment for manifold learning, which can be cast into two categories by their motivations.

- Methods based on evaluating how well the rank of neighbor samples, according to pairwise Euclidean distances, is preserved within each local neighborhood.
- Methods based on evaluating how well each local neigh-

P. Zhang is with the Data Center, National Disaster Reduction Center of China, Beijing, P.R. China (e-mail: zhangpeng@ndrcc.gov.cn).

Y. Ren is with the Career Center, Tsinghua University, Beijing, P.R. China.

B. Zhang is with the LSEC and the Institute of Applied Mathematics, AMSS, Chinese Academy of Sciences, Beijing 100190, China.

neighborhood matches its corresponding embedding under rigid motion.

These methods are proved to be useful to isometric manifold learning methods, such as ISOMAP and RML. However, a large variety of manifold learning methods output normalized embeddings, such as LLE, HLLE, LE, LTSA and MVU, just to name a few. In these method, embeddings have unit variance up to a global scale factor. Then the distance rank of neighbor samples is disturbed in the embedding as pairwise Euclidean distances are no longer preserved. Meanwhile, anisotropic coordinate scaling caused by normalization can not be recovered by rigid motion. As a consequence, existent methods would report false quality assessments for normalized embeddings.

In this paper, we first propose a new measure, named Anisotropic Scaling Independent Measure (ASIM), which can efficiently compare the similarity between two configurations under rigid motion and anisotropic coordinate scaling. Then based on ASIM, we propose a novel embedding quality assessment method, named Normalization Independent Embedding Quality Assessment (NIEQA), which can efficiently assess the quality of normalized embeddings quantitatively. The NIEQA method owns three characteristics.

- 1) NIEQA can be applied to both isometric and normalized embeddings. Since NIEQA uses ASIM to assess the similarity between patches in high-dimensional input space and their corresponding low-dimensional embeddings, the distortion caused by normalization can be eliminated. Then even if the aspect ratio of a learned embedding is scaled, NIEQA can still give faithful evaluation of how well the geometric structure of data manifold is preserved.
- 2) NIEQA can provide both local and global assessments. NIEQA consists of two components for embedding quality assessment, a global one and a local one. The global assessment evaluates how well the skeleton of a data manifold, represented by a set of landmark points, is preserved, while the local assessment evaluates how well local neighborhoods are preserved. Therefore, NIEQA can provide an overall evaluation.
- 3) NIEQA can serve as a natural tool for model selection and evaluation tasks. Using NIEQA to provide quantitative evaluations on learned embeddings, we can select optimal parameters for a specific method and compare the performance among different methods.

In order to evaluate the performance of NIEQA, we conduct a series of experiments on benchmark data sets, including both synthetic and real-world data. Experimental results on these data sets validate the effectiveness of the proposed method.

TABLE I
MAIN NOTATIONS.

\mathbb{R}^n	n -dimensional Euclidean space where high-dimensional data samples lie
\mathbb{R}^m	m -dimensional Euclidean space, $m < n$, where low-dimensional embeddings lie
x_i	The i -th data sample in \mathbb{R}^n , $i = 1, 2, \dots, N$
\mathcal{X}	$\mathcal{X} = \{x_1, x_2, \dots, x_N\}$
X	$X = [x_1 \ x_2 \ \dots \ x_N]$, $n \times N$ data matrix
\mathcal{X}_i	$\mathcal{X}_i = \{x_{i_1}, x_{i_2}, \dots, x_{i_k}\}$, local neighborhood of x_i
X_i	$X_i = [x_{i_1} \ x_{i_2} \ \dots \ x_{i_k}]$, $n \times k$ data matrix
$\mathcal{N}_k(x_i)$	The index set of the k nearest neighbors of x_i in \mathcal{X}
y_i	low-dimensional embedding of x_i , $i = 1, 2, \dots, N$
\mathcal{Y}	$\mathcal{Y} = \{y_1, y_2, \dots, y_N\}$
Y	$Y = [y_1 \ y_2 \ \dots \ y_N]$, $m \times N$ data matrix
\mathcal{Y}_i	$\mathcal{Y}_i = \{y_{i_1}, y_{i_2}, \dots, y_{i_k}\}$, low-dimensional embedding of \mathcal{X}_i
Y_i	$Y_i = [y_{i_1} \ y_{i_2} \ \dots \ y_{i_k}]$, $m \times k$ data matrix
$\mathcal{N}_k(y_i)$	The index set of the k nearest neighbors of y_i in \mathcal{Y}
e_k	$e = [1 \ 1 \ \dots \ 1]^T$, k dimensional column vector of all ones
I_k	Identity matrix of size k
$\ \cdot\ _2$	L_2 norm for a vector
$\ \cdot\ _F$	Frobenius norm for a matrix

The rest of the paper is organized as follows. A literature review on related works is presented in Section II. The Anisotropic Scaling Independent Measure (ASIM) is described in Section III. Then the Normalization Independent Embedding Quality Assessment (NIEQA) method is depicted in Section IV. Experimental results are reported in Section V. Some concluding remarks as well as outlooks for future research are given in Section VI.

II. LITERATURE REVIEW ON RELATED WORKS

In this section, the current state-of-the-art on embedding quality assessment methods are reviewed. For convenience and clarity of presentation, main notations used in this paper are summarized in Table I. Throughout the whole paper, all data samples are in the form of column vectors. The superscript of a data vector is the index of its component.

According to motivation and application range, existent embedding quality assessment methods can be categorized into two groups: local approaches and global approaches. Related works in the two categories are reviewed respectively as follows.

A. Local approaches

Goldberg and Ritov [23] proposed the Procrustes Measure (PM) that enables quantitative comparison of outputs of isometric manifold learning methods. For each \mathcal{X}_i and \mathcal{Y}_i , their method first uses Procrustes analysis [24]–[26] to find an

optimal rigid motion transformation, consisting of a rotation and a translation, after which \mathcal{Y}_i best matches \mathcal{X}_i . Then the local similarity is computed as

$$L(X_i, Y_i) = \sum_{j=1}^k \|x_{i_j} - Ry_{i_j} - b\|_2^2,$$

where R and t are the optimal rotation matrix and translation vector, respectively. Finally, the assessment is given by

$$M_P = \frac{1}{N} \sum_{i=1}^N L(X_i, Y_i) / \|H_k X_i\|_F^2, \quad (1)$$

where $H_k = I_k - e_k e_k^T$.

An M_P close to zero suggests a faithful embedding. Reported experimental results show that the PM method provides good estimation of embedding quality for isometric methods such as ISOMAP. However, as pointed out by the authors, PM is not suitable for normalized embedding since the geometric structure of every local neighborhood is distorted by normalization. Although a modified version of PM is proposed in [23], which eliminates global scaling of each neighborhood, it still can not address the issue of sperate scaling of coordinates in the low-dimensional embedding.

Besides the PM method, a series of works follow the line that a faithful embedding would yield a high degree of overlap between the neighbor sets of a data sample and of its corresponding embedding. Several works are proposed by using different ways to define the overlap degree. A representative one is the LC meta-criteria (LCMC) proposed by Chen and Buja [27], [28], which can serve as a diagnostic tool for measuring local adequacy of learned embedding. The LCMC assessment is defined as the sum of local overlap degree and given by

$$M_{LC} = \frac{1}{kN} \sum_{i=1}^N |\mathcal{N}_k(x_i) \cap \mathcal{N}_k(y_i)|. \quad (2)$$

Venna and Kaski [29] proposed an assessment method which consists of two measures, one for trustworthiness and one for continuity, based on the change of indices of neighbor samples in \mathbb{R}^n and R^m according to pairwise Euclidean distances, respectively. Aguirre *et al.* proposed an alternative approach for quantifying the embedding quality, by evaluating the possible overlaps in the low-dimensional embedding. Their assessment is used for automatic choice of the number of nearest neighbors for LLE [30] and also exploited in [31] to evaluate the embedding quality of LLE with optimal regularization parameter. Akkucuk and Carroll [32] independently developed the Agreement Rate (AR) metric which shares the same form to M_{LC} . Based on AR, they suggested another useful assessment method called corrected agreement rate, by

randomly reorganize the indices of data in \mathcal{Y} . Also with AR, France and Carroll [33] proposed a method using the RAND index to evaluate dimensionality reduction methods.

Lee and Verleysen [34], [35] proposed a general framework, named co-ranking matrix, for rank-based criteria. The aforementioned methods, which are based on distance ranking of local neighborhoods, can all be cast into this unified framework. The block structure of the co-ranking matrix also provides an intuitive way to visualize the differences between distinct methods. In [36], they further extended their work to circumvent the global scale dependency.

The above assessments based on overlap degrees of neighborhoods are implemented in the same way: an embedding with good quality corresponds to a high value of the assessment. They work well for isometric embeddings since pairwise distances within each neighborhood are preserved. However, when the embedding is normalized, the neighborhood structure is distorted since pairwise distances are no longer kept. The overlap degree would be much lower than expected even if the embedding is of high quality under visual inspection.

B. Global approaches

Tenenbaum *et al.* [7] suggested to use the residual variance as a diagnostic measure to evaluate the embedding quality. Given \mathcal{X} and \mathcal{Y} , the residual variance is computed by

$$M_{RV} = 1 - \rho^2(G_X, D_Y), \quad (3)$$

where $\rho(G_X, D_Y)$ is the standard linear correlation coefficients taken over all entries of G_X and D_Y . Here $G_X(i, j)$ is the approximated geodesic distance between x_i and x_j [7] and $D_Y(i, j) = \|y_i - y_j\|_2$. A low value of M_{RV} close to zero indicates a good equality of the embedding.

The M_{RV} measure was applied to choose the dimension of learned embedding for ISOMAP [7] and the optimal parameter for LLE [37]. Nevertheless, for a normalized embedding the geodesic distances are no longer preserved and the reliability of M_{RV} may decrease in such case.

Dollár *et al.* [38] proposed a supervised method for model evaluation problem of manifold learning. They assume that there is a very large ground truth data set containing the training data. Pairwise geodesic distances are approximated within this set using ISOMAP, and the assessment is defined as the average error between pairwise Euclidean distances in the embedding and corresponding geodesic distances. However, in real situations we do not usually have such ground truth set and their assessment can not be used in general cases.

Recently, Meng *et al.* proposed a new quality assessment criterion to encode both local-neighborhood-preserving and

global-structure-holding performances for manifold learning. In their method, a shortest path tree is first constructed from the k -NN neighborhood graph of training data. Then the global assessment is computed by using Spearman’s rank order correlation coefficient defined on the rankings of branch lengths. Finally, the overall assessment is defined to be a linear combination of the global assessment and M_{LC} . In their work, normalization is treated as a negative aspect in quality assessment, while our work is to define a new assessment which is independent of normalization.

III. ASIM: ANISOTROPIC SCALING INDEPENDENT MEASURE

In this section, we introduce a novel measure, named Anisotropic Scaling Independent Measure (ASIM), which can effectively evaluate the similarity between two configurations under rigid motion and anisotropic coordinate scaling. A synthetic example is first given in Subsection III-A to demonstrate why existent assessments fail under normalization. Then the motivation and overall description of ASIM are presented in Subsection III-B. Finally, the computational details are stated in Subsection III-C.

A. A synthetic example

We randomly generate 100 points within the area $[-2, 2] \times [-1, 1]$ in \mathbb{R}^2 , which form the input data set $\mathcal{X} = \{x_1, x_2, \dots, x_{100}\}$. Next we normalize \mathcal{X} to get output data \mathcal{Y} such that $YY^T = I_2$, which are taken as the embedding of \mathcal{X} . In fact, \mathcal{X} can be obtained from \mathcal{Y} through a rotation and anisotropic coordinate scaling, that is, $X = RSY$ where

$$R = \begin{pmatrix} -0.9991 & 0.0434 \\ 0.0434 & 0.0991 \end{pmatrix}, \quad S = \begin{pmatrix} 11.6414 & 0 \\ 0 & 5.6236 \end{pmatrix}.$$

In Fig. 1(a), $x_i, i = 1, 2, \dots, 100$ are marked with blue dots and the 10 nearest neighbors of the origin in \mathcal{X} are marked with blue circles. In Fig. 1(b), $y_i, i = 1, 2, \dots, 100$ are marked with red dots and the 10 nearest neighbors of the origin in \mathcal{Y} are marked with red squares. Meanwhile, the corresponding embeddings of the 10 nearest neighbors of the origin in \mathcal{X} are marked with blue circles. From Fig. 1(b) we can see that the neighborhood of the origin change a lot after normalization. Only 6 nearest neighbors are still in the neighborhood after normalization and the overlap degree is only 60%. Meanwhile, we also compute the Procrustes measure M_P between \mathcal{X} and \mathcal{Y} and show it in Fig. 1(b). After normalization, M_P is as high as 0.8054.

Through this synthetic example, we can clearly observe the distortion on M_P and local neighborhood overlap degree caused by normalization.

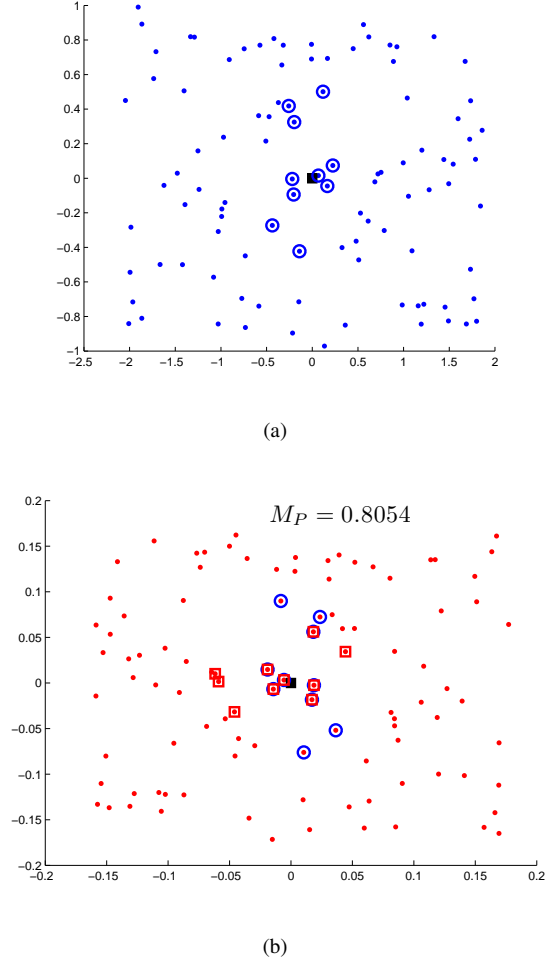


Fig. 1. A synthetic example where existent assessments fail. (a) Input data \mathcal{X} , marked by blue dots. (b) Normalized embedding \mathcal{Y} , marked by red dots. Black filled square: the origin $(0, 0)^T$. Blue circles: the k nearest neighbors of the origin in \mathcal{X} and their corresponding embeddings. Red squares: the k nearest neighbors of the origin in \mathcal{Y} .

B. Motivation and description of ASIM

Since a manifold is a topological space which is locally equivalent to a Euclidean subspace, an embedding would be *faithful* if it preserves the structure of local neighborhoods. Then we face a question that how to define the “preservation” of local neighborhood structure.

Under the assumption that the data manifold is *dense*, each local neighborhood \mathcal{X}_i can be roughly viewed as a linear subspace embedded in the ambient space. Considering possible normalization on \mathcal{Y} , a rational and reasonable choice is to define a new measure which can efficiently assess the similarity between \mathcal{X}_i and \mathcal{Y}_i under rigid motion and anisotropic coordinate scaling.

Formally, for each index i , we assume that there exists a rigid motion and anisotropic coordinate scaling between \mathcal{X}_i and \mathcal{Y}_i . Since a rigid motion can be decomposed into a rotation

and a translation, then for any $x_{i_j} \in \mathcal{X}_i$ we assume that

$$x_{i_j} = P_i D_i y_{i_j} + t_i, \quad (4)$$

where $P_i \in \mathbb{R}^{n \times m}$ is orthogonal, that is, $P_i^T P_i = I_m$. D_i is a diagonal matrix of rank m and $t_i \in \mathbb{R}^n$ stands for an arbitrary translation.

To evaluate how similar \mathcal{X}_i and \mathcal{Y}_i are, our goal is to find optimal P_i^* , D_i^* and t_i^* such that \mathcal{Y}_i best matches \mathcal{X}_i under Eq. (4). Equivalently, we need to solve the following constrained optimization problem

$$\begin{aligned} \min \quad & \sum_{j=1}^k \|x_{i_j} - P_i^* D_i^* y_{i_j} - t_i^*\|_2^2 \\ \text{s. t.} \quad & P_i^{*T} P_i^* = I_m \\ & D_i \in \mathcal{D}(m) \end{aligned}, \quad (5)$$

where $\mathcal{D}(m)$ is the set of all diagonal matrices of rank m .

Then the neighborhood ‘‘preservation’’ degree can be defined as the sum of squared distances between corresponding samples in \mathcal{X}_i and \mathcal{Y}_i under the above transformation. Formally, the anisotropic scaling independent measure (ASIM) is defined as follows

$$M_{asim}(X_i, Y_i) = \frac{\sum_{j=1}^k \|x_{i_j} - P_i^* D_i^* y_{i_j} - t_i^*\|_2^2}{\sum_{j=1}^k \|x_{i_j}\|_2^2}, \quad (6)$$

or in matrix form

$$M_{asim}(X_i, Y_i) = \|X_i - P_i^* D_i^* Y_i - t_i^* e_k^T\|_F^2 / \|X_i\|_F^2, \quad (7)$$

where the normalization item in denominator is introduced to eliminate arbitrary scaling.

C. Computation of ASIM

The optimization problem Eq. (5) does not admit a closed-form solution. Alternatively, we use gradient descent method to solve Eq. (5). Note that all $n \times m$ orthogonal matrices form the so-called Stiefel manifold, which is a Riemannian submanifold embedded in \mathbb{R}^{nm} . We denote this manifold by $St(n, m)$. Also note that $\mathcal{D}(m)$ is closed for matrix addition, multiplication and scalar multiplication, hence $\mathcal{D}(m)$ is homeomorphic to \mathbb{R}^m . Then Eq. (5) can be resolved by using gradient descent method over matrix manifolds.

For convenience of presentation, we first introduce the δ operator [39], which is defined as follows

Definition 1. When the δ operator is defined on a n -dimensional vector $v = (v_1, v_2, \dots, v_n)^T$, $\delta(v)$ is a $n \times n$ diagonal matrix whose diagonal entries are just components of v , that is

$$\delta(v) = \begin{pmatrix} v_1 & & & \\ & v_2 & & \\ & & \ddots & \\ & & & v_n \end{pmatrix}.$$

When the δ operator is defined on a $n \times n$ square matrix $A = (a_{ij})$, $\delta(A)$ is a n -dimensional vector formed by the diagonal entries of v , that is,

$$\delta(A) = (a_{11}, a_{22}, \dots, a_{nn})^T.$$

The δ operator can be compounded, which yields

$$\delta^2(v) = v$$

$$\delta^2(A) = \begin{pmatrix} a_{11} & & & \\ & a_{22} & & \\ & & \ddots & \\ & & & a_{nn} \end{pmatrix}.$$

With the above notations, Eq. (5) now can be rewritten in matrix form as

$$\begin{aligned} \min_{P_i, D_i, t_i} \quad & \|X_i - P_i D_i Y_i - t_i e_k^T\|_F^2 \\ \text{s. t.} \quad & P_i \in St(n, m), D_i \in \mathcal{D}_m. \end{aligned} \quad (8)$$

Next, we solve Eq. (8) in three steps, which are described respectively as follows.

1) *Computation t_i^** : Let $L_i = P_i D_i$ and note that for any matrix A , $\|A\|_F^2 = \text{tr}(A^T A)$. Then the objective function can be written as

$$f(L_i, t_i) = \text{tr}((X_i - L_i Y_i - t_i e_k^T)^T (X_i - L_i Y_i - t_i e_k^T)). \quad (9)$$

By using the propositions of matrix trace Eq. (9) can be expanded as

$$\begin{aligned} f(L_i, t_i) = & \text{tr}(X_i^T X_i) + \text{tr}(Y_i^T L_i^T L_i Y_i) - \\ & 2 \text{tr}(Y_i X_i^T L_i) + \text{tr}(t_i e_k^T e_k t_i^T) - \\ & 2 \text{tr}(e_k^T X_i^T t_i) + \text{tr}(e_k^T Y_i^T L_i^T t_i). \end{aligned} \quad (10)$$

Taking derivative with respect to t_i yields

$$\frac{\partial f(L_i, t_i)}{\partial t_i} = 2k t_i - 2X_i e_k + 2L_i Y_i t_i.$$

Since $f(L_i, t_i)$ is a strict convex function of t_i , then by making both sides of the above equation to be zero, we can get the optimal solution to t_i as follows

$$t_i^* = \frac{1}{k} (X_i - P_i D_i Y_i) e_k. \quad (11)$$

Substitute t_i^* into Eq. (8), and the latter one is rewritten as

$$\begin{aligned} \min_{P_i, D_i} \quad & \|\bar{X}_i - P_i D_i \bar{Y}_i\|_F^2 \\ \text{s. t.} \quad & P_i \in St(n, m), D_i \in \mathcal{D}_m, \end{aligned} \quad (12)$$

where $\bar{X}_i = X_i (I_k - \frac{1}{k} e_k e_k^T)$ and $\bar{Y}_i = Y_i (I_k - \frac{1}{k} e_k e_k^T)$.

2) *Computation of D_i^** : In the second step, we compute the optimal solution D_i^* to D_i with respect to P_i . Let $A_i = \bar{Y}_i \bar{Y}_i^T$ and $B_i = P^T \bar{X}_i \bar{Y}_i^T$, and denote the objective function in Eq. (12) by $f(P_i, D_i)$. Then we have

$$\begin{aligned} f(P_i, D_i) &= \text{tr}(D^2 A_i) - 2 \text{tr}(D B_i) + \text{tr}(\bar{X}_i \bar{X}_i^T) \\ &= \sum_{j=1}^m a_{jj}^{(i)} (d_j^{(i)})^2 - 2 \sum_{j=1}^m b_{jj}^{(i)} d_j^{(i)} + \text{tr}(\bar{X}_i \bar{X}_i^T), \end{aligned}$$

where $a_{jj}^{(i)}$, $b_{jj}^{(i)}$ and $d_j^{(i)}$ are the j -th diagonal entries of A_i , B_i and D_i , respectively.

Since $a_{jj}^{(i)} \geq 0$, $j = 1, 2, \dots, m$, f is a convex function of vector $\delta(D_i)$. Taking partial derivative with respect to $d_j^{(i)}$ ($j = 1, 2, \dots, m$) and by making them to be zero, we can get the global optimal solutions to $d_j^{(i)}$ ($j = 1, 2, \dots, m$) as follows

$$d_j^{(i)} = \frac{b_{jj}^{(i)}}{a_{jj}^{(i)}}, \quad j = 1, 2, \dots, m.$$

Then D_i^* is given by

$$D_i^* = (\delta^2(A_i))^{-1} \delta^2(B_i). \quad (13)$$

Substituting Eq. (13) into f yields

$$\begin{aligned} f(P_i) &= \text{tr}(A_i ((\delta^2(A_i))^{-1} \delta^2(B_i))^2) - \\ &\quad 2 \text{tr}((\delta^2(A_i))^{-1} \delta^2(B_i) B_i) + \text{tr}(\bar{X}_i \bar{X}_i^T) \\ &= \sum_{j=1}^m a_{jj}^{(i)} \frac{(b_{jj}^{(i)})^2}{(a_{jj}^{(i)})^2} - 2 \sum_{j=1}^m b_{jj}^{(i)} \frac{b_{jj}^{(i)}}{a_{jj}^{(i)}} + \text{tr}(\bar{X}_i \bar{X}_i^T) \\ &= - \sum_{j=1}^m \frac{(b_{jj}^{(i)})^2}{a_{jj}^{(i)}} + \text{tr}(\bar{X}_i \bar{X}_i^T). \end{aligned}$$

Let $M_i = \bar{X}_i \bar{Y}_i^T (\delta^2(A_i))^{-1/2}$, then $f(P_i)$ can be rewritten as

$$\begin{aligned} f(P_i) &= - \sum_{j=1}^m (P_i^T M_{i_j})^2 + \text{tr}(\bar{X}_i \bar{X}_i^T) \\ &= - \text{tr}((P_i^T M_i) \odot (P_i^T M_i)) + \text{tr}(\bar{X}_i \bar{X}_i^T), \end{aligned}$$

where P_{i_j} and M_{i_j} are the j -th columns of matrices P_i and M_i , respectively. \odot stands for the Hadamard product over matrices. The optimization problem Eq. (12) can be transformed into

$$\begin{aligned} \max_{P_i} \quad & \phi(P_i) = \text{tr}((P_i^T M_i) \odot (P_i^T M_i)) \\ \text{s. t.} \quad & P_i \in \text{St}(n, m). \end{aligned} \quad (14)$$

3) *Computation of P_i^** : In the third step, we use gradient descent method over matrix manifold to solve Eq. (14), which is an optimization problem for matrix function over the Stiefel manifold $\text{St}(n, m)$.

Denote the gradient of ϕ in \mathbb{R}^{nm} by $\nabla \bar{\phi}(P_i)$ and the gradient of ϕ on $\text{St}(n, m)$ by $\nabla \phi(P_i)$, then by the proposition

of Stiefel manifold [40], $\nabla \phi(P_i)$ is the projection of $\nabla \bar{\phi}(P_i)$ onto the tangential space at P_i and can be computed by the following formula

$$\nabla \phi(P_i) = \nabla \bar{\phi}(P_i) - P_i \frac{P_i^Z \nabla \bar{\phi}(P_i) + (\nabla \bar{\phi}(P_i))^T P_i}{2}. \quad (15)$$

Now all we need is to compute $\nabla \bar{\phi}(P_i)$. Let $F(P_i) = (P_i^T M_i) \odot (P_i^T M_i)$. From matrix calculus, the differentiation of ϕ with respect to P_i is

$$D\phi(P_i) = (\text{vec } I_m)^T DF(P_i), \quad (16)$$

where the vec operator reformulates a $n \times m$ matrix into a nm -dimensional vector by stacking its columns one underneath other.

Next we derive $DF(P_i)$. First, we have

$$dF(P_i) = 2(M_i^T P_i) \odot (M_i^T dP_i) = 2W_m^T ((M_i^T P_i) \otimes (M_i^T dP_i)) W_m,$$

where \otimes stands for the Kronecker product over matrices and $W_m = (\text{vec } w_1 w_1^T, \text{vec } w_2 w_2^T, \dots, \text{vec } w_m w_m^T)$ is an $m^2 \times m$ matrix. w_i , $i = 1, 2, \dots, m$ is an m -dimensional vector who has 1 in its i -th component and 0 elsewhere. Then we have

$$\begin{aligned} \text{vec } dF(P_i) &= 2 \text{vec}(W_m^T ((M_i^T P_i) \otimes (M_i^T dP_i)) W_m) \\ &= 2(W_m^T \otimes W_m) \text{vec}(M_i^T P_i \otimes (M_i^T dP_i)) \\ &= 2(W_m^T \otimes W_m) (H_i \otimes I_m) \text{vec}(M_i^T dP_i) \\ &= 2(W_m^T \otimes W_m) (H_i \otimes I_m) (I_m \otimes M_i^T) d \text{vec } P_i, \end{aligned}$$

where $H_i = ((I_m \otimes K_{mm})((\text{vec } M_i^T P_i) \otimes I_m)) \otimes I_m$. Here K_{mm} is a permutation matrix of order m^2 , and for any square matrix M of order m , $K_{mm} \text{vec } M = \text{vec } M^T$. Then by matrix calculus [41], we have

$$DF(P_i) = 2(W_m^T \otimes W_m) (H_i \otimes I_m) (I_m \otimes M_i^T).$$

Furthermore, through algebraic deduction and Eq. (16), we have

$$D\phi(P_i) = (\text{vec } I_m)^T DF(P_i) = 2 \text{vec}(M_i \delta^2(P_i^T M_i))^T.$$

Then $\nabla \bar{\phi}(P_i)$ is given by the following formula

$$\nabla \bar{\phi}(P_i) = 2M_i \delta^2(P_i^T M_i),$$

and by using Eq. (15), $\nabla \phi(P_i)$ now reads

$$\nabla \phi(P_i) = 2M_i \delta^2(P_i^T M_i) - P_i P_i^T \delta^2(P_i^T M_i) - P_i \delta^2(P_i^T M_i) M_i^T P_i. \quad (17)$$

Given a step length for iteration, we apply gradient descent method to find P_i^* such that $\nabla \phi(P_i)$ vanishes. In each iteration, we first update P_i as

$$\tilde{P}_i = P_i + \alpha \nabla \phi(P_i).$$

Then we retract \tilde{P}_i to $\text{St}(n, m)$. From the property of $\text{St}(n, m)$, such retraction can be obtained through the QR

Algorithm 1: Anisotropic Scaling Independent Measure (ASIM), M_{asim} .

Input: Local neighborhood matrix X_i and corresponding embedding matrix Y_i , number of nearest neighbors k , step length for iteration α , and threshold ϵ for stopping criterion.

Output: $M_{asim}(X_i, Y_i)$.

Step 1. Assign $\bar{X}_i = X_i(I_k - e_k e_k^T)$.

Step 2. Assign $\bar{Y}_i = Y_i(I_k - e_k e_k^T)$.

Step 3. Set initial value $P_i^{(0)}$ for P_i .

Step 4. Use Eq. (17) to compute $\nabla\phi(P_i^{(0)})$.

Step 5. If $\|\nabla\phi(P_i^{(0)})\|_F < \epsilon$, goto Step 6; otherwise, do

$$P_i^{(0)} \leftarrow P_i^{(0)} + \alpha \nabla\phi(P_i^{(0)}) .$$

Compute the QR decomposition of $P_i^{(0)}$, $P_i^{(0)} = Q_i R_i$.

Let $P_i^{(0)} \leftarrow Q_i$ and goto Step 5.

Step 6. Let $P_i^* = P_i^{(0)}$ and use Eq. (13) to compute D_i^* .

Step 7. Use Eq. (11) to compute t_i^* . Step 8. Compute

$M_{asim}(X_i, Y_i)$ through Eq. (7).

decomposition of \tilde{P}_i . Let $\tilde{P}_i = Q_i R_i$, where $Q_i \in St(n, m)$ and R_i is an upper-triangular matrix. The retraction of \tilde{P}_i to $St(n, m)$ is just Q_i .

In each iteration, we use Q_i to update P_i until $\|\nabla\phi(P_i)\|_F$ is less than a given threshold ϵ . After P_i^* is computed, D_i^* can be given by Eq. (13), and the optimal value to Eq. (12) is $f(P_i^*, D_i^*)$.

4) *The algorithm and discussion:* Finally, we summarize the computation process of M_{asim} in Algorithm 1.

When the dimension n of input samples is very high, performing QR decomposition of \tilde{P}_i in each iteration will greatly increase of computational complexity of Algorithm 1. A possible solution to this issue is first projecting \mathcal{X}_i to its tangential space, denoted as $T\mathcal{X}_i$, and then computing $M_{asim}(T\mathcal{X}_i, Y_i)$. When data are densely distributed on the manifold, $T\mathcal{X}_i$ can optimally recover the local linear structure of a manifold. Therefore, such strategy is feasible. The tangential space can be approximated by using PCA, MDS or the method proposed in [42].

IV. NORMALIZATION INDEPENDENT EMBEDDING QUALITY ASSESSMENT

When assessing the quality of embeddings, we need to consider both local and global evaluations. This leads to two issues.

- Does the embedding preserve the global topology of the manifold?

- Does the embedding preserve the geometric structure of local neighborhood neighborhoods?

In this section, we propose Normalization Independent Embedding Quality Assessment method (NIEQA) to address these two issues, which is independent of normalization. NIEQA is based on the ASIM measure stated in Section III and consists of two assessments, a local one and a global one. In the following subsections, we introduce these two assessments respectively as well as how NIEQA can be implemented in model selection and model evaluation.

A. Local assessment

For local neighborhood \mathcal{X}_i on a data manifold and its corresponding low-dimensional embedding \mathcal{Y}_i , the local measure M_{asim} defined in last section characterizes how well local neighborhood structure is preserved and is independent of normalization. Therefore, we define the local assessment as the mean value of $M_{asim}(X_i, Y_i)$ over index i , that is,

$$M_L(X, Y) = \frac{1}{N} \sum_{i=1}^N M_{asim}(X_i, Y_i) . \quad (18)$$

B. Global assessment

From geometric intuition, if an embedding preserves the global topology of the data manifold well, then such embedding should preserve relative positions among “representative” samples on the manifold. In other words, if we treat these “representative” samples as a local neighborhood, where pairwise Euclidean distances among neighborhood samples are replaced with pairwise geodesic distances on the manifold, then a good embedding should preserve the geometric structure of this neighborhood.

Motivated by the above consideration, we define the global assessment as the matching degree between the aforementioned described neighborhood and its corresponding embedding under rigid motion and anisotropic coordinate scaling.

The computation of the global assessment consists of three steps, which are depicted below, respectively.

- 1) **Selecting landmark points.** First, for each training sample x_i , find its k_l nearest neighbors. Treat x_i as a node in a graph and add edges among neighboring samples with edge length being pairwise Euclidean distance. Through such construction we get a connected graph. Then we use the shortest path length between x_i and x_j to approximate the geodesic distance between them for all i and j . Next, we count how many shortest paths going through each x_i and record this number as its importance degree. Finally, the top 10% most

important data samples are selected as landmark points on the manifold and the set they formed is denoted by \mathcal{X}_l .

- 2) **Computing $\tilde{\mathcal{Y}}_l$.** Once \mathcal{X}_l is fixed in the first step, the distance between any two landmark points is defined to be the approximated geodesic distance. Then we implement MDS [4] to \mathcal{X}_l to obtain its isometric embedding $\tilde{\mathcal{Y}}_l$, which optimally preserve relative positions of landmark points on the manifold. Note that the dimensions of $\tilde{\mathcal{Y}}_l$ and \mathcal{Y}_l are equal, and the latter one is the subset in \mathcal{Y} corresponding to \mathcal{X}_l .
- 3) **Computing the global assessment.** We define the global assessment M_G to be the ASIM measure between $\tilde{\mathcal{Y}}_l$ and \mathcal{Y}_l

$$M_G(X, Y) = M_{asim}(\tilde{Y}_l, Y_l), \quad (19)$$

where \tilde{Y}_l and Y_l are the $m \times l$ data matrices corresponding to $\tilde{\mathcal{Y}}_l$ and \mathcal{Y}_l , respectively.

Remark 1. During landmark points selection, the parameter k_l needs to be set manually. Based on experimental experience, setting $k_l = 0.1N$ can yield a connected graph that approximates the manifold structure well. However, if the graph is disconnected under current k_l , k_l should be set to be the smallest integer which makes the graph fully connected.

The landmark points selection method stated above has intuitive geometric motivation and is easy to implement. It can also be replaced with other more accurate yet more complicated approaches, for example, the methods proposed in [43] and [44].

C. Implementation in model evaluation and model selection

In this subsection, we state how to implement the NIEQA method to model evaluation and model selection for manifold learning.

- **Model evaluation.** Given X , suppose that we have two embeddings, namely Y_1 and Y_2 , obtained by different manifold learning methods. Then we say that Y_1 owns better locality preservation than Y_2 if $M_L(X, Y_1) < M_L(X, Y_2)$ and vice versa. We say Y_1 owns better global topology preservation than Y_2 if $M_G(X, Y_1) < M_G(X, Y_2)$ and vice versa.
- **Model selection.** Given X and a set of parameters $\mathcal{P} = \{p_1, p_2, \dots, p_l\}$, for each parameter p_i we compute its corresponding embedding $Y^{(i)}$ using specific manifold learning method. Then we use M_G or M_L or their combination, which depends on the user's demand, to evaluate the quality of $Y^{(i)}$. Finally, the p_i corresponding

TABLE II
DESCRIPTION OF EXPERIMENTAL DATA SETS.

Data manifold	N	n	m	Description
Swissroll	1000	3	2	Surface isometrically embedded in \mathbb{R}^3
Swisshole	1000	3	2	Surface embedded in \mathbb{R}^3
Gaussian	1000	3	2	Surface isometrically embedded in \mathbb{R}^3
l1eface	1493	560	2	Face manifold with resolution 28×20

TABLE III
NOTATIONS USED IN EXPERIMENTS.

Notation	Description
M_P	Procrustes measure (Eq. (1)) [23]
M_P^c	M_P with global scaling removed [23]
M_{LC}	LCMC measure (Eq. (2)) [27], [28]
M_{RV}	Residual Variance measure (Eq. (3)) [7]
M_L	Local assessment of NIEQA (Eq. (18))
M_G	Global assessment of NIEQA (Eq. (19))
M_t	Matching degree between \mathcal{Y} and ground truth \mathcal{U} , $M_{asim}(Y, U)$

to the lowest assessment score is chosen to be the optimal parameter.

V. EXPERIMENTS

In this section, the effectiveness of the NIEQA method is validated through a series of experimental tests on benchmark data sets. In Subsection V-A, NIEQA is applied to model evaluation for manifold learning. In Subsection V-A, NIEQA is used to select optimal parameters for the LTSA method which outputs normalized embeddings. In experiments, NIEQA is compared with three commonly used assessment methods. We compute $1 - M_{LC}$ instead M_{LC} to obtain a unified criterion, that is, a small assessment value close to zero indicates good quality of the embedding. The benchmark data sets used in experiments are briefly depicted in Table II and notations for methods are summarized in Table III.

A. Model evaluation

In the first experiment, we apply NIEQA to model evaluation of the `Swissroll` manifold with parameter equation

$$\begin{cases} x^1 &= u^1 \cos u^1 \\ x^2 &= u^2 \\ x^3 &= u^1 \sin u^1 \end{cases}.$$

We use LLE [5], LE [10], LTSA [14], ISOMAP [7] and RML [16] to learn this manifold, respectively. 1000 training samples are randomly generated and the number of nearest

neighbors is 10. Figs. 2 (c)-(g) shows the results of manifold learning, where \mathcal{X} and \mathcal{U} stands for the training data and the groundtruth of intrinsic degrees of freedom, respectively. By visual inspection, the embeddings given by LTSA and RML are the most similar to \mathcal{U} . The one given by ISOMAP is a litter worse, and the one learned by LLE has a great change in global shape. LE fails to recover the geometric structure of \mathcal{U} .

For embeddings given by the above methods, we compute the different assessments described in Table III and use bar plots to visualize their values in Figs. 2(h)-(m). From the bar plots, we can see that M_P only works for isometric embeddings given by ISOMAP and RML while reports false high values for normalized embeddings learned by LTSA and LLE. Although M_P^c eliminates the affects of global scaling, only the scale of M_P is normalized and it still reports false high values for normalized embeddings. M_{LC} and M_{RV} fails to output reasonable equality evaluations. It should be noted that M_{RV} is originally designed for the ISOMAP method and hence works well for the embedding given by ISOMAP.

The two assessments M_L and M_G in NIEQA provide overall and reasonable evaluations on embedding quality for various methods. M_L shows that LTSA and RML best preserve local neighborhood. LLE and ISOMAP perform worse, and LE performs the worst. M_G further indicates that the global-shape-preservation of the embedding given by LLE is not good. This completely matches visual inspection, which demonstrates that NIEQA can effectively evaluate the quality of both isometric and normalized embeddings.

Besides, the bar plot of the matching degree M_t between \mathcal{Y} and \mathcal{U} is shown in Fig. 2(n). We can see that only M_L and M_G match M_t , which validates the effectiveness of NIEQA.

Similar to the first experiment, we apply NIEQA to model evaluation of the `Swisshole` manifold, which shares the same parameter equation to `Swissroll`. The difference is that the set of intrinsic degree of freedoms \mathcal{U} is no longer a convex set, where a rectangular region in \mathcal{U} is digged out. Therefore, `Swisshole` manifold is geodesic non-connected. 1000 training samples are randomly generated from the manifold and the number of nearest neighbors k is 10. The learned low-dimensional embeddings and the bar plots of quality assessments are shown in Fig. 3.

From Fig. 3, we can see that LTSA and RML correctly learned the geometric structure of \mathcal{U} with the highest quality over other approaches. The embedding given by LLE has a distortion in global shape. ISOMAP and LE fails to learn the structure of \mathcal{U} . From the bar plots in Figs. 3 (h)-(l), we can see that M_L reports a reasonable quality assessment and matches

M_t well which is illustrated in Fig. 3(m). M_P and M_P^c works only for isometric embeddings provided by ISOMAP and RML. M_{LC} and M_{RV} fails to report reasonable evaluations. Since `Swisshole` manifold is geodesic non-connected, using shortest path length would fail to approximate geodesic distance. Therefore, we do not compute the global assessment M_G in NIEQA.

In the third experiment, we apply NIEQA to model evaluation of the `Gaussian` manifold, whose parameter equation is

$$\begin{cases} x^1 = u^1 \\ x^2 = u^2 \\ x^3 = (1/2\pi) \exp\{-((u^1)^2 + (u^2)^2)/2\} \end{cases}.$$

1000 training samples are randomly generated from the manifold and the number of nearest neighbors k is 10. Fig. 4 shows the learned low-dimensional embeddings as well as bar plots of different quality assessments.

From Fig. 4, we can observe that except LE all the other methods successfully learned the geometric structure of this manifold, whilst the quality of the embedding given by ISOMAP is a litter worse. From Figs. 4 (h)-(m), we can see that M_P^c performs well in this case by eliminating the global scaling factor. This is due to the isotropic property of this manifold. M_{LC} reports correct evaluations but still leans against to RML. M_{RV} fails to assess the embeddings correctly. Both the two assessments in NIEQA successfully evaluate the quality of different embeddings and match M_t well. Note that the `Gaussian` surface is isotropic, hence the measure M_P^c also works. However, for anisotropic surfaces like `Swissroll` and `Swisshole`, only removing global scaling would not yield a reasonable assessment.

In the next experiment, we apply NIEQA to model evaluation tasks on the `l1eface` data set, which is a high-dimensional image manifold. As the code of RML on high-dimensional data is not available, we do not test RML on this data set. The training data contain 1965 face images, and the intrinsic degrees of freedom are the angle of face orientation and the variation of facial emotion. We randomly select 1493 images as training data such that the data graph constructed via ISOMAP is connected. We apply LLE, LE, ISOMAP and LTSA to learn this manifold with 15 nearest neighbors. The two dimensional embeddings learned by these methods and bar plots of the quality assessments given by different methods are shown in Fig. 5.

From Fig. 5 we can see that the embedding given by LLE does not recover the change of face orientation. The other methods all successfully extract the two intrinsic degrees of freedom despite the difference in embedding shape. The

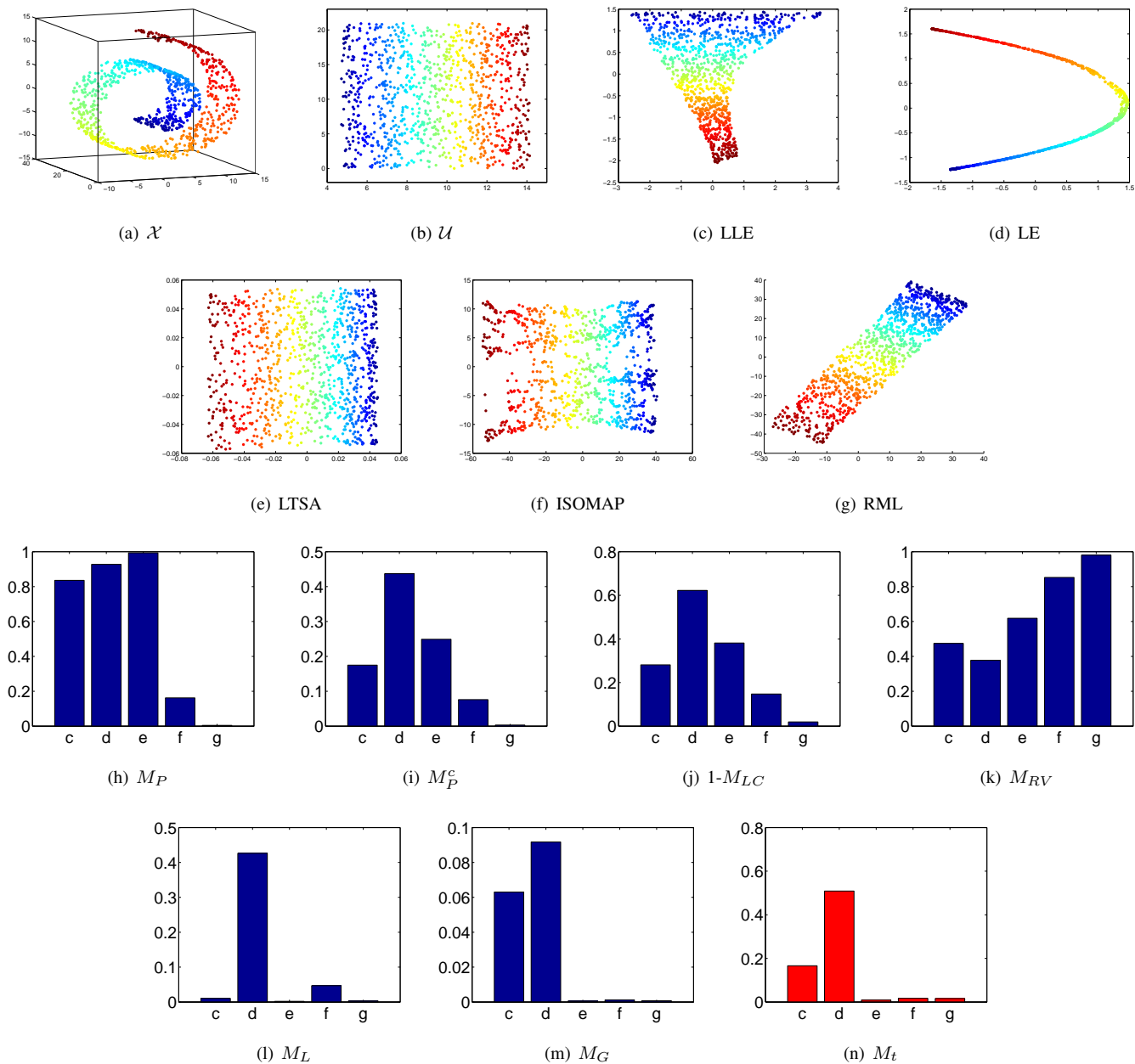


Fig. 2. Manifold learning results on *Swissroll*. (a) Training data \mathcal{X} . (b) Groundtruth of intrinsic degrees of freedom \mathcal{U} . (c)-(g) Embeddings learned by various method. The name of each method is stated below each subfigure. (h)-(n) Bar plots of different assessments on learned embeddings. The lower-case character under each bar corresponds to the index of the subfigure above.

above visual inspection is also validated by the bar plots of quantitative assessments shown in Figs. 5(e)-(i). M_{LC} , M_{RV} and M_L all suggest that the quality of the embedding given by LLE is poor, while the others are almost of the same quality. M_{LC} and M_L indicate that the embedding given by LTSA is of the highest quality. M_P and M_P^c fail in this case.

Remark 2. In experiments on high-dimensional image manifold, we did not compute M_G . The reason lies in that the computation of M_G needs to estimate geodesic distances based on shortest graph paths. However, we have no prior knowledge

on the underlying geometric structure of image manifolds, hence using M_G to assess the global topology would yield unknown bias. Also note that the values of intrinsic degrees of freedom for image manifolds are unknown, hence we do not compute M_t either.

B. Model selection

In this subsection, we take the LTSA method as an example to demonstrate the application of NIEQA to model selection task. The most important parameter for LTSA is the number of nearest neighbors k . We first apply NIEQA to selecting k

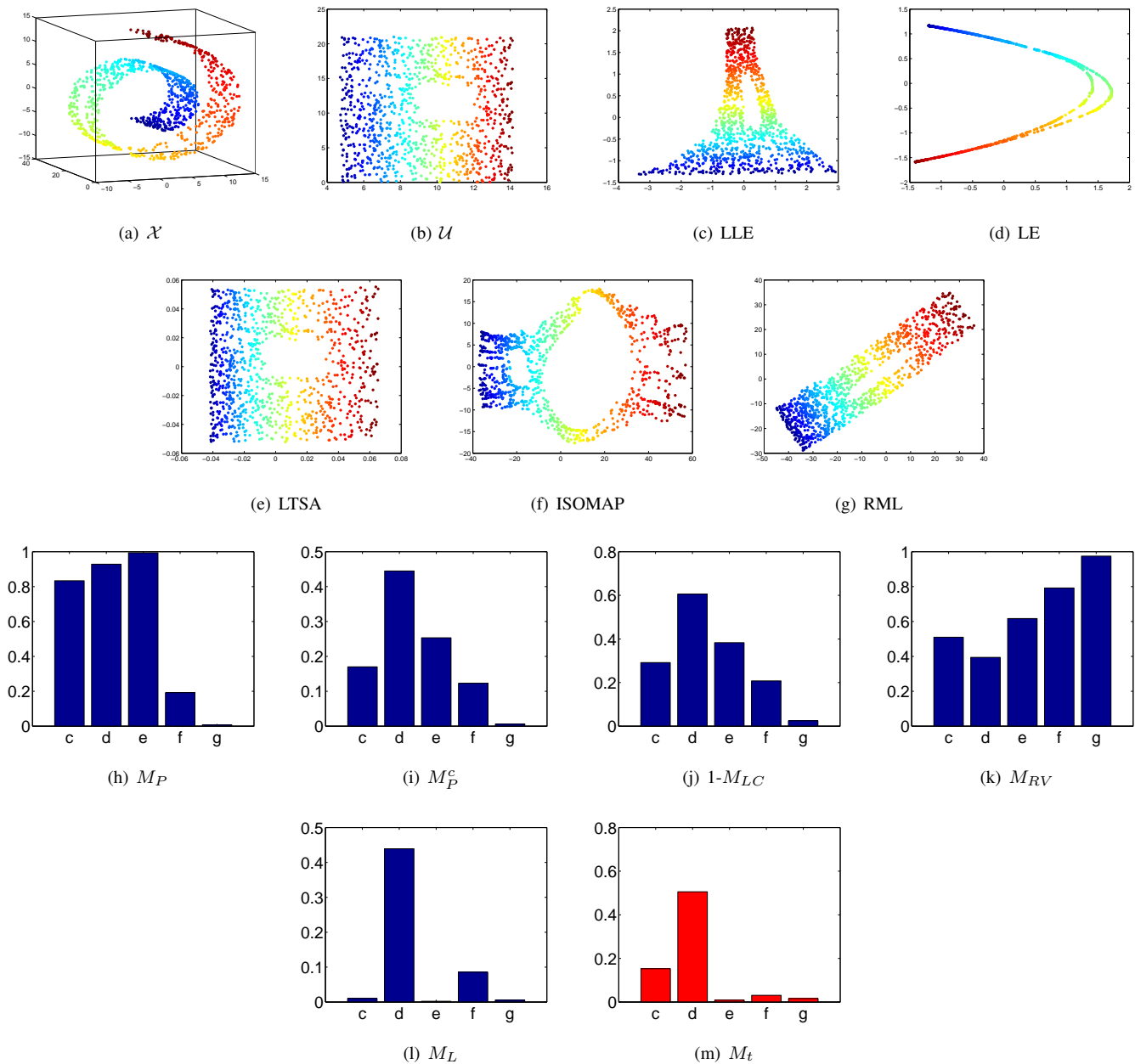


Fig. 3. Manifold learning results on *Swissroll*. (a) Training data \mathcal{X} . (b) Groundtruth of intrinsic degrees of freedom \mathcal{U} . (c)-(g) Embeddings learned by various method. The name of each method is stated below each subfigure. (h)-(m) Bar plots of different assessments on learned embeddings. The lower-case character under each bar corresponds to the index of the subfigure above.

for LTSA on the *Swissroll* data set. Similar to the first experiment in Section V-A. We randomly select 1000 samples from the *Swissroll* manifold as training data. The values of k are chosen to be integers from 5 to 24. For each k , an embedding is learned with LTSA, which are shown in Fig. 6. The assessments given by NIEQA corresponding to different values of k are shown in Fig. 8(a). From the figure we can see that when k is taking values between 6 and 15, LTSA would produce embeddings with high quality. This observation is also supported by visual inspection from Fig. 6, which validates the effectiveness of the NIEQA method.

In the second experiment, we apply NIEQA to select optimal k for LTSA on the *l1eface* data set. Training data are the same to those used in the experiment in Section V-A. Values of k are taken to be integers from 5 to 24. For each k , an embedding is learned with LTSA, which is shown in Fig. 7. Corresponding quality assessment given by NIEQA are illustrated in Fig. 8(b), from which we can see that the embedding corresponding to $k = 14$ is of the highest quality. We can also observe that when $k > 8$, the quality of embeddings improves along with the increase of k , which is also validated by visual inspections from Fig. 7.

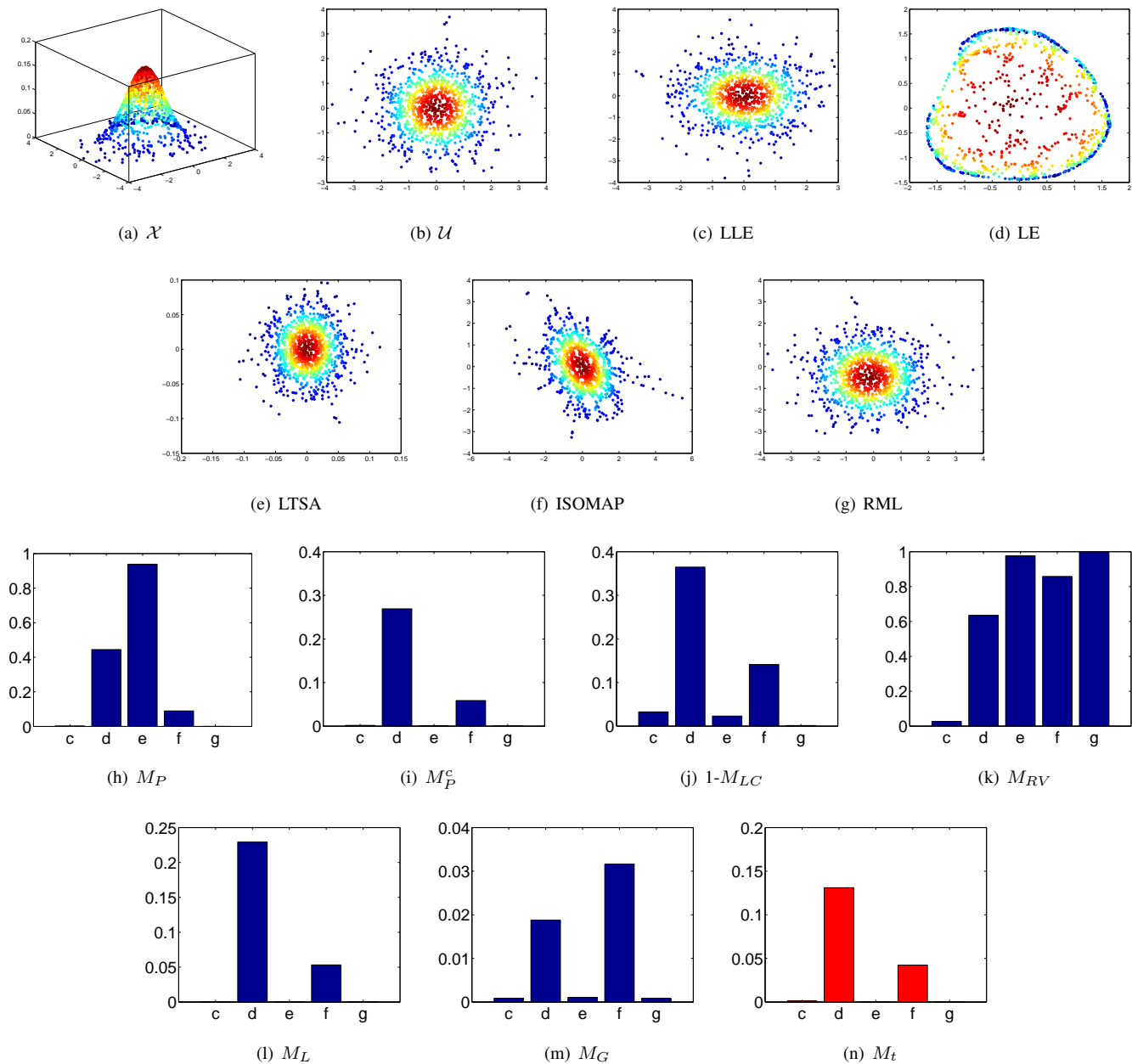


Fig. 4. Manifold learning results on Gaussian. (a) Training data \mathcal{X} . (b) Groundtruth of intrinsic degrees of freedom \mathcal{U} . (c)-(g) Embeddings learned by various method. The name of each method is stated below each subfigure. (h)-(n) Bar plots of different assessments on learned embeddings. The lower-case character under each bar corresponds to the index of the subfigure above.

VI. CONCLUSIONS AND DISCUSSIONS

In this paper, we proposed a novel normalization independent embedding quality assessment (NIEQA) method for manifold learning, which has wider application range than current approaches. We first propose a new local measure, which can quantitatively evaluate how well local neighborhood structure is preserved under rigid motion and anisotropic coordinate scaling. Then the NIEQA method, which is designed based on this new measure, can effectively and quantitatively evaluate the quality of both isometric and normalized embeddings. Fur-

thermore, the NIEQA method considers both local and global topology, thus it can yield an overall assessment. Experimental tests on benchmark data sets validate the effectiveness of the proposed method.

Some discussions and possible improvements in future works are stated below.

- The measure M_{asim} is computed by using gradient descent method on matrix manifold. Whether the solution converges to a global optima remains unproved and is the key part of our future works. Meanwhile, we will also consider how to design more efficient iteration method

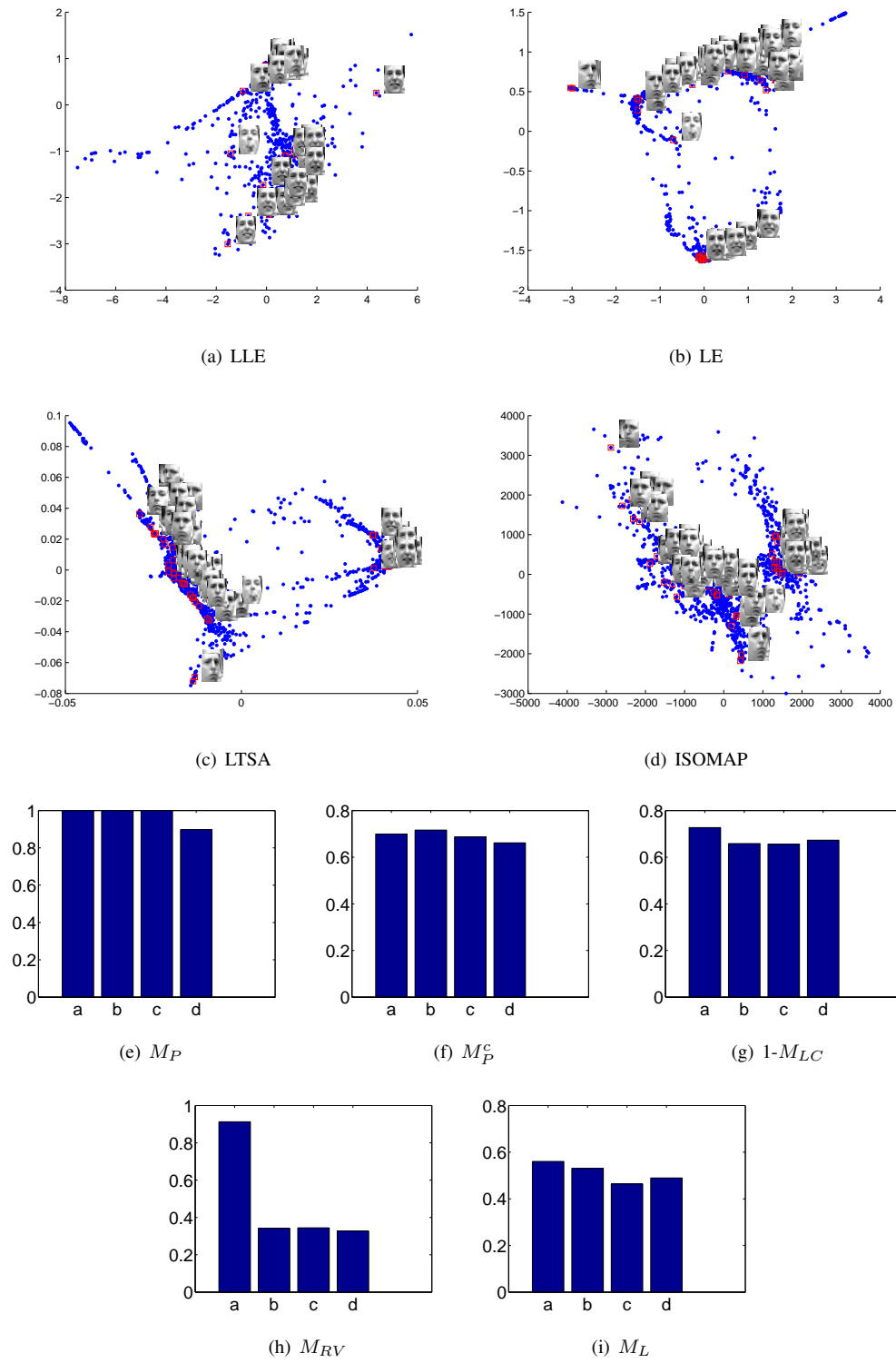


Fig. 5. Manifold learning results on `l1eface`. (a)-(d) Embeddings learned by various methods. The name of each method is stated below each subfigure. (e)-(i) Bar plots of different assessments on learned embeddings. The lower-case character under each bar corresponds to the index of the subfigure above.

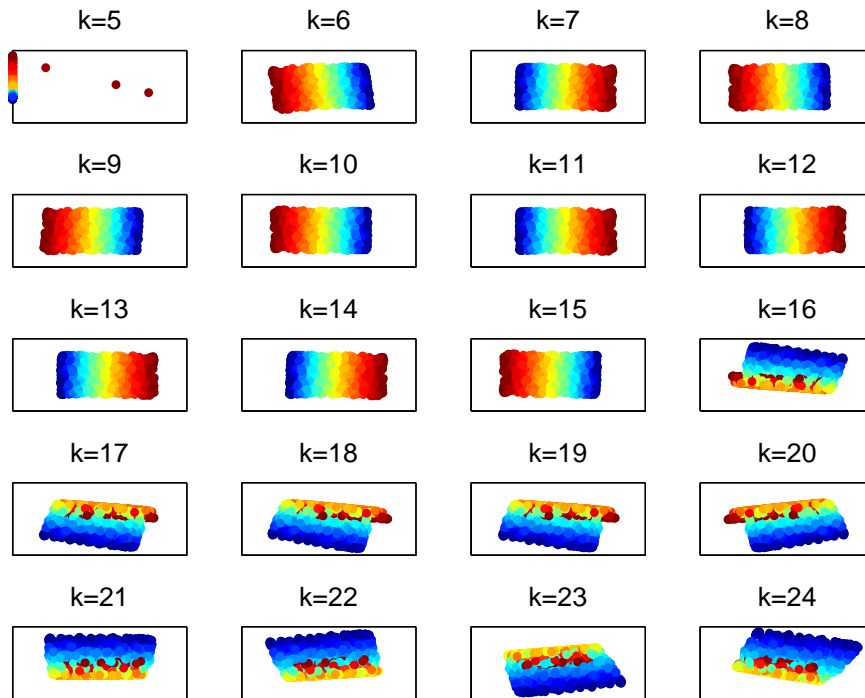


Fig. 6. Embeddings given by LTSA on `Swissroll` data set with different values of k .

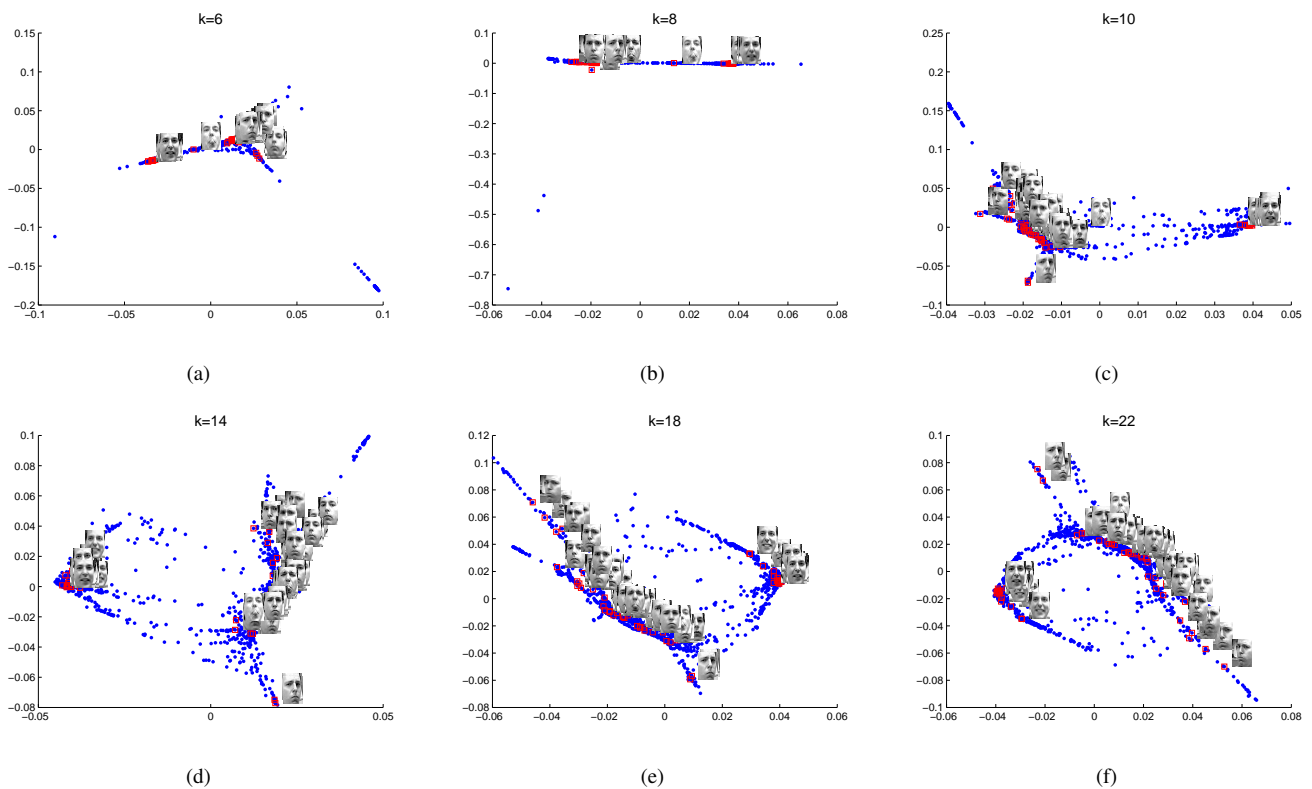


Fig. 7. Embeddings given by LTSA on `11eface` data set with different values of k .

to accelerate convergence.

- The NIEQA method is based on a local matching methodology. Its basic assumption is that the manifold is densely sampled and training data strictly lie on the manifold. For data manifold with noise or outliers, the efficiency of NIEQA may be affected. A possible solution to this issue is to implement denoising or outlier removal process before training.
- Based on NIEQA, whether we can design a manifold learning method with better learning performance is also one of our future works.

ACKNOWLEDGEMENTS

This work was partly supported by the NNSF of China grant no. 90820007, and the 973 Program of China grant no. 2007CB311002.

REFERENCES

- [1] D. L. Donoho, High-dimensional data analysis: the curses and blessings of dimensionality, in: *Proceedings of American Mathematical Society Conference on Math Challenges of the 21st Century*, 2000.
- [2] M. Turk, A. Pentland, Eigenfaces for recognition, *Journal of Cognitive Neuroscience* 3 (1) (1991) 71–86.
- [3] I. T. Jolliffe, *Principal Component Analysis*, 2nd Edition, Springer, 2002.
- [4] T. F. Cox, M. A. A. Cox, *Multidimensional Scaling*, Second Edition, Chapman & Hall, 2000.
- [5] S. T. Roweis, L. K. Saul, Nonlinear dimensionality reduction by locally linear embedding, *Science* 290 (5500) (2000) 2323–2326.
- [6] L. K. Saul, S. T. Roweis, Think globally, fit locally: Unsupervised learning of low dimensional manifolds, *Journal of Machine Learning Research* 4 (2003) 119–155.
- [7] J. B. Tenenbaum, V. Silva, J. C. Langford, A global geometric framework for nonlinear dimensionality reduction, *Science* 290 (5500) (2000) 2319–2323.
- [8] V. De Silva, J. B. Tenenbaum, Global versus local methods in nonlinear dimensionality reduction, in: *Advances in Neural Information Processing Systems* 15, Vol. 15, 2003, pp. 705–712.
- [9] M. Belkin, *Problems of learning on manifolds*, Ph.D. thesis, The University of Chicago (2003).
- [10] M. Belkin, P. Niyogi, Laplacian eigenmaps for dimensionality reduction and data representation, *Neural Computation* 15 (6) (2003) 1373–1396.
- [11] D. L. Donoho, C. Grimes, Hessian eigenmaps: Locally linear embedding techniques for high-dimensional data, *Proceedings of the National Academy of Sciences of the United States of America* 100 (10) (2003) 5591–5596.
- [12] R. R. Coifman, S. Lafon, A. B. Lee, M. Maggioni, B. Nadler, F. Warner, S. W. Zucker, Geometric diffusions as a tool for harmonic analysis and structure definition of data: Diffusion maps, *Proceedings of the National Academy of Sciences of the United States of America* 102 (21) (2005) 7426–7431.
- [13] S. Lafon, A. B. Lee, Diffusion maps and coarse-graining: A unified framework for dimensionality reduction, graph partitioning, and data set parameterization, *IEEE Transactions on Pattern Analysis and Machine Intelligence* 28 (9) (2006) 1393–1403.
- [14] Z. Zhang, H. Zha, Principal manifolds and nonlinear dimensionality reduction via tangent space alignment, *SIAM Journal on Scientific Computing* 26 (1) (2005) 313–338.
- [15] K. Weinberger, L. Saul, Unsupervised learning of image manifolds by semidefinite programming, *International Journal of Computer Vision* 70 (1) (2006) 77–90.
- [16] T. Lin, H. Zha, Riemannian manifold learning, *IEEE Transactions on Pattern Analysis and Machine Intelligence* 30 (5) (2008) 796–809.
- [17] L. Wang, D. Suter, Learning and matching of dynamic shape manifolds for human action recognition, *IEEE Transactions on Image Processing* 16 (6) (2007) 1646–1661.
- [18] J. Chen, R. Wang, S. Yan, S. Shan, X. Chen, W. Gao, Enhancing human face detection by resampling examples through manifolds, *IEEE Transactions on Systems, Man and Cybernetics, Part A: Systems and Humans* 37 (6) (2007) 1017–1028.
- [19] M. Cheng, M. Ho, C. Huang, Gait analysis for human identification through manifold learning and hmm, *Pattern Recognition* 41 (8) (2008) 2541–2553.
- [20] Y. Cheon, D. Kim, Natural facial expression recognition using differential-aam and manifold learning, *Pattern Recogn.* 42 (7) (2009) 1340–1350.
- [21] C. M. Bachmann, T. L. Ainsworth, R. A. Fusina, Exploiting manifold geometry in hyperspectral imagery, *IEEE Transactions on Geoscience and Remote Sensing* 43 (3) (2005) 441–454.
- [22] H. Qiao, P. Zhang, B. Zhang, S. Zheng, Learning an intrinsic-variable preserving manifold for dynamic visual tracking, *IEEE Transactions on Systems, Man and Cybernetics, Part B: Cybernetics* 40 (3) (2010) 868–880.
- [23] Y. Goldberg, Y. Ritov, Local procrustes for manifold embedding: a measure of embedding quality and embedding algorithms, *Machine Learning* 77 (1) (2009) 1–25.
- [24] R. Sibson, Studies in robustness of multidimensional-scaling: Procrustes statistics, *Journal of the Royal Statistical Society Series B - Methodological* 40 (2) (1978) 234–238.
- [25] R. Sibson, Perturbational analysis of classical scaling, *Journal of the Royal Statistical Society Series B - Methodological* 41 (2) (1979) 217–229.
- [26] G. A. F. Seber, *Multivariate observations*, John Wiley & Sons. INC, 2004.
- [27] L. S. Chen, *Local multidimensional scaling for nonlinear dimension reduction, graph layout and proximity analysis*, Ph.D. thesis, University of Pennsylvania (2006).
- [28] L. Chen, A. Buja, Local multidimensional scaling for nonlinear dimension reduction, graph drawing, and proximity analysis, *Journal of the American Statistical Association* 104 (485) (2009) 209–219.
- [29] J. Venna, S. Kaski, Local multidimensional scaling, *Neural Networks* 19 (6-7) (2006) 889–899.
- [30] J. Valencia-Aguirre, A. Álvarez Mesa, G. Daza-Santacoloma, G. Castellanos-Domínguez, Automatic choice of the number of nearest neighbors in locally linear embedding, in: *CIARP '09: Proceedings of the 14th Iberoamerican Conference on Pattern Recognition*, 2009, pp. 77–84.
- [31] G. Daza-Santacoloma, C. D. Acosta-Medina, G. Castellanos-Domínguez, Regularization parameter choice in locally linear embedding, *Neurocomputing* 73 (10-12) (2010) 1595–1605.
- [32] U. Akkucuk, J. D. Carroll, Paramap vs. isomap: A comparison of two nonlinear mapping algorithms, *Journal of Classification* 23 (2006) 221–254.
- [33] S. France, D. Carroll, Development of an agreement metric based upon the rand index for the evaluation of dimensionality reduction techniques, with applications to mapping customer data, in: *Machine Learning and Data Mining in Pattern Recognition*, Vol. 4571 of *Lecture Notes in Computer Science*, Springer Berlin / Heidelberg, 2007, pp. 499–517.
- [34] J. A. Lee, M. Verleysen, Quality assessment of dimensionality reduction: Rank-based criteria, *Neurocomputing* 72 (7-9) (2009) 1431–1443.
- [35] J. A. Lee, M. Verleysen, Quality assessment of nonlinear dimensionality reduction based on k-ary neighborhoods, in: *Journal of Machine*

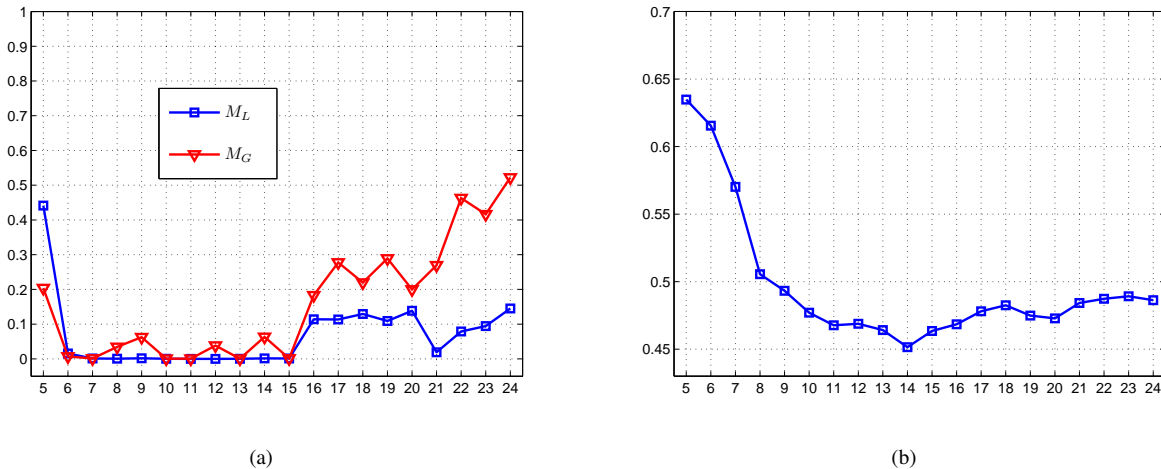


Fig. 8. Graph plot of embedding quality assessments in model selection experiment for the LTSA method. (a) Assessments on `Swissroll` data set with different value of k . (b) Assessment M_L on `l1eface` data set with different value of k .

Learning Research: Workshop and Conference proceedings, 2008, pp. 21–35.

- [36] J. A. Lee, M. Verleysen, Scale-independent quality criteria for dimensionality reduction, *Pattern Recognition Letters* 31 (2010) 2248–2257.
- [37] O. Kouropteva, O. Okun, M. Pietikäinen, Selection of the optimal parameter value for the locally linear embedding algorithm, in: *The 1st International Conference on Fuzzy Systems and Knowledge Discovery*, 2002, pp. 359–363.
- [38] P. Dollár, V. Rabaud, S. Belongie, Non-isometric manifold learning: analysis and an algorithm, in: *ICML '07: Proceedings of the 24th international conference on Machine learning*, ACM, New York, NY, USA, 2007, pp. 241–248.
- [39] J. Dattorro, *Convex Optimization & Euclidean Distance Geometry*, Meboo Publishing USA, 2005.
- [40] P.-A. Absil, R. Mahony, R. Sepulchre, *Optimization Algorithms on Matrix Manifolds*, Princeton University Press, Princeton, NJ, USA, 2007.
- [41] J. R. Magnus, H. Neudecker, *Matrix differential calculus with applications in statistics and econometrics*, 2nd Edition, John Wiley & Sons, 1999.
- [42] P. Zhang, H. Qiao, B. Zhang, An improved local tangent space alignment method for manifold learning, *Pattern Recognition Letters* 32 (2) (2011) 181–190.
- [43] V. d. Silva, J. B. Tenenbaum, Selecting landmark points for sparse manifold learning, in: *Advances in Neural Information Processing Systems (NIPS)*, Vol. 18, 2006, pp. 1241–1248.
- [44] J. Li, P. Hao, Finding representative landmarks of data on manifolds, *Pattern Recogn.* 42 (11) (2009) 2335–2352.